# Tree-Ring Reconstruction of Single-Day Precipitation Totals over Eastern Colorado

IAN M. HOWARD AND DAVID W. STAHLE

*Department of Geosciences, University of Arkansas, Fayetteville, Arkansas*

(Manuscript received 15 April 2019, in final form 24 October 2019)

ABSTRACT

Mean daily to monthly precipitation averages peak in late July over eastern Colorado and some of the most damaging Front Range flash floods have occurred because of extreme 1-day rainfall events during this period. Tree-ring chronologies of adjusted latewood width in ponderosa pine from eastern Colorado are highly correlated with the highest 1-day rainfall totals occurring during this 2-week precipitation maximum in late July. A regional average of four adjusted latewood chronologies from eastern Colorado was used to reconstruct the single wettest day observed during the last two weeks of July. The regional chronology was calibrated with the CPC 0.25° × 0.25° Daily U.S. Unified Gauge-Based Analysis of Precipitation dataset and explains 65% of the variance in the highest 1-day late July precipitation totals in the instrumental data from 1948 to 1997. The reconstruction and instrumental data extend fully from 1779 to 2019 and indicate that the frequency of 1-day rainfall extremes in late July has increased since the late eighteenth century. The largest instrumental and reconstructed 1-day precipitation extremes are most commonly associated with the intrusion of a major frontal system into a deep layer of atmospheric moisture across eastern Colorado. These general synoptic conditions have been previously linked to extreme localized rainfall totals and widespread thunderstorm activity over Colorado during the summer season. Chronologies of adjusted latewood width in semiarid eastern Colorado constitute a proxy of weather time-scale rainfall events useful for investigations of long-term variability and for framing natural and potential anthropogenic forcing of precipitation extremes during this 2-week precipitation maximum in a long historical perspective.

## 1. Introduction

Extreme rainstorms during the summer period of late July and early August have caused some of the most damaging flash floods to impact the Colorado Front Range, including the catastrophic floods at Big Thompson Canyon on 31 July 1976 (Maddox et al. 1978), and at Spring Creek near Fort Collins, Colorado, on 27–28 July 1997 (Doesken and McKee 1998). Heavy precipitation and major flash flooding in Colorado can occur throughout the year (McKee and Doesken 1997), famously including Denver's "flood of record" in June 1965 (Matthai 1969) and the flooding of September 2013 over northern Colorado (Gochis et al. 2015). But the Front Range and High Plains of Colorado are especially vulnerable to extreme precipitation and flash flooding in summer when the advection of subtropical moisture and relatively weak upper-level steering winds can result in slow-moving thunderstorms capable of producing significant hourly and daily rainfall totals (Maddox et al. 1978; McKee and Doesken 1997; Cotton et al. 2003). The frequency and intensity of extreme rainfall events appear to have increased over the United States since 1901 (Kunkel et al. 2013; Wuebbles et al. 2017) and the positive trend has been most pronounced in summer (Karl and Knight 1998). However, there is less evidence for changes to extreme precipitation over Colorado (Hoerling et al. 2013; Lukas et al. 2014; Mahoney et al. 2018), due in part to the greater natural variability of climate in the Southwest (Lukas et al. 2014; Mahoney et al. 2018). While global climate model simulations suggest that the frequency and magnitude of daily rainfall extremes may increase with unabated anthropogenic global warming (Kunkel et al. 2013; Wuebbles et al. 2017; Mahoney et al. 2018), there is large uncertainty associated with changes in extreme summer rainfall events in Colorado (Alexander et al. 2013). Historical documentary evidence, early instrumental observations, and potentially exactly dated wood anatomical or subannual tree-ring width data might provide a longer historical perspective on midsummer rainfall extremes prior to the onset of heavy anthropogenic weather and climate forcing.

Climate sensitive tree-ring chronologies have been widely used to reconstruct growing season precipitation

*Corresponding author*: Ian M. Howard, ihowardksu@gmail.com

DOI: 10.1175/MWR-D-19-0114.1

and the Palmer drought severity index (PDSI; Palmer 1965; Stahle and Cleaveland 1992; Fritts 2001; Cook et al. 2007). Douglass (1920) described tree growth as a response to integrated climate conditions ''distributed throughout the year.'' The correlation between annual precipitation totals and tree-ring chronologies can in fact be so high that they have been referred to as ''integrating pluviometers'' (Blasing and Fritts 1976). Because tree growth tends to use soil moisture accumulated during or even preceding the growing season, it has not been possible to develop estimates of daily time-scale weather phenomena on a continuous year-by-year basis extending back into prehistory using total ring-width chronologies. Weather extremes associated with severe growing season freeze events (LaMarche and Hirschboeck 1984; Stahle 1990; Bräuning et al. 2016; Barbosa et al. 2019) and midgrowing season weather reversals (Villalba and Veblen 1996; Fritts 2001; Edmondson 2010) may induce distinctive anatomical evidence in the xylem cells of living trees. The meteorological significance of these so-called frost and false ring chronologies can be demonstrated during the instrumental period and then used to infer the history of these episodic events during the preinstrumental era. But weather sufficiently extreme to cause anatomical damage to tree rings is infrequent, so the derived event chronologies tend to be highly discontinuous in time.

In this article we describe the strong correlation between the single wettest 24-h period during late July (19 July–1 August) and a regional tree-ring chronology based on the last-formed latewood cells of ponderosa pine (*Pinus ponderosa*), the so-called ''adjusted latewood width'' chronology (hereafter referred to as simply ''latewood,'' ''adjusted latewood,'' or ''LWa''). This peak 2-week period in midsummer is climatologically the wettest time of the year over eastern Colorado based on average 2-week precipitation totals. The regional adjusted latewood chronology is also highly correlated with total monthly precipitation in July over an area of eastern Colorado (37.75°–39.75°N, 105°–103°W), but higher correlations are computed when the latewood data are compared only with the wettest 24-h rainfall interval during late July. The exact Julian date of these 24-h rainfall extremes vary from year to year, but for the available ponderosa pine chronologies they appear to be largely confined to the period from 19 July to 1 August. These largest rainfall days also constitute the majority of the full 2-week total precipitation for midsummer in eastern Colorado, and we use the strong single-day signal in adjusted latewood width data to reconstruct the wettest 24-h totals each year from 1779 to 1997. These ''dendrometeorological'' rainfall proxies are then used along with instrumental observations to describe the synoptic meteorology and long-term changes in midsummer rainfall extremes, placing them in the context of natural weather and climate variability since the late eighteenth century.

### *Warm season precipitation climatology in eastern Colorado*

Warm season (April–September) precipitation contributes over 70% of the annual total in the semiarid Front Range and adjacent High Plains of eastern Colorado (Mahoney et al. 2015). However, a substantial fraction of the April–September total tends to occur during two periods when daily precipitation rates are highest (Fig. 1). Averaged across the eastern Colorado study region (black box on the map of the United States in Fig. 1), these spring (May) and midsummer (late July) rainfall maxima are separated by a drier early summer period that reaches a minimum on Julian day 182 (1 July). For much of eastern Colorado the timing of the annual precipitation maximum usually occurs in late July and early August, but in the northern parts of the study region the highest daily precipitation rates tend to occur in late spring. The gridded daily data may also underestimate the spring precipitation peak because the daily totals are calculated for the period 1200–1200 UTC (Chen et al. 2008) and maximum 24-h precipitation during the spring season may extend across over two days more often than in summer.

Higher daily precipitation rates in spring are generally associated with the passage of synoptic-scale storm systems that transport moisture from the Gulf of Mexico northwestward into eastern Colorado. The larger secondary peak in late July can partly be attributed to the Great Plains low-level jet that advects Gulf moisture on the western sector of a persistent ridge that commonly develops in summer over the central United States (Tang and Reiter 1984). The low pressure system related to the North American monsoon system can also funnel moist mid- to upper-level air as far northward as Colorado and southern Wyoming, particularly during late July and early August (Hales 1974; Tang and Reiter 1984). Pulses of subtropical moisture from these two sources, combined with factors such as the topography of the Rocky Mountains, daytime heating of the land surface, and the passage of weak synoptic disturbances embedded in the upper-level flow, result in localized convective thunderstorms that can be a near daily occurrence from early summer through as late as September (McKee and Doesken 1997). Certain configurations of atmospheric circulation over the United States, combined with additional forcing from strong frontal systems and upper-level synoptic shortwaves, can enhance the advection of subtropical moisture and

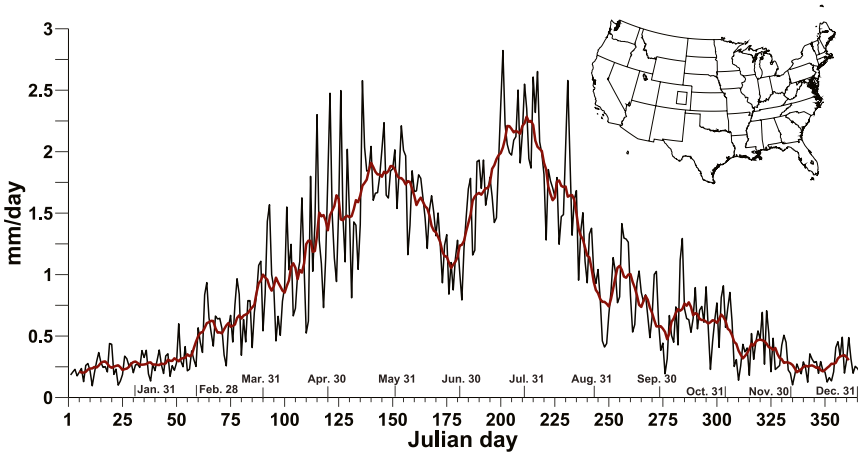


FIG. 1. The daily mean precipitation totals for 1948–2019 are plotted for a regional average of eastern Colorado from the CPC 0.25° × 0.25° Daily U.S. Unified Gauge-Based Analysis of Precipitation dataset (37.75°–39.75°N, 105°–103°W; black box on the map inset). The red line is a 10-day moving average of the daily means. Note the two peaks in the climatology of daily rainfall during late spring and late July.

create thermodynamic conditions that have been responsible for some of the largest hourly and daily rainfall totals recorded in Colorado during this 2-week peak in precipitation during the summer months.

## 2. Data and methods

### *a. Daily rainfall data*

The gridded daily precipitation data used in this study were acquired from the National Oceanic and Atmospheric Administration (NOAA) Climate Prediction Center (CPC) 0.25° × 0.25° Daily U.S. Unified Gauge-Based Analysis of Precipitation dataset (Chen et al. 2008). The gridded daily data were calculated using the optimal interpolation algorithm described by Xie et al. (2007), which utilizes a dense network of observing sites to calculate daily precipitation values on a 0.25° latitude by 0.25° longitude grid extending from 1948 to 2005, with real-time observations provided from 2006 to the present. The daily totals at each grid point are based on the 24 h accumulation of precipitation ending at 1200 UTC of the current day. The daily precipitation data were extracted for an area of eastern Colorado (black box in Fig. 2). This 2.0° × 2.0° region was selected because the daily, biweekly, and monthly precipitation totals calculated for this study area tended to have the highest correlation with the tree-ring data compared to other domains. Rarely do the individual grids points in the eastern Colorado study region contain zero values due to the nature of the interpolated data. For the purposes of this study, we treated daily precipitation values of less than 1 mm as zero at each grid point.

Daily precipitation totals from 40 selected observation stations in eastern Colorado in the Global Historical Climatology Network (GHCN) from the National Climatic Data Center (NCDC) were also used for analyses with the gridded daily data and tree-ring chronologies (Fig. 2). These 40 stations were selected based on their location within or near the eastern Colorado study region (Fig. 2), and the availability of at least 25 years of continuous observations of late July

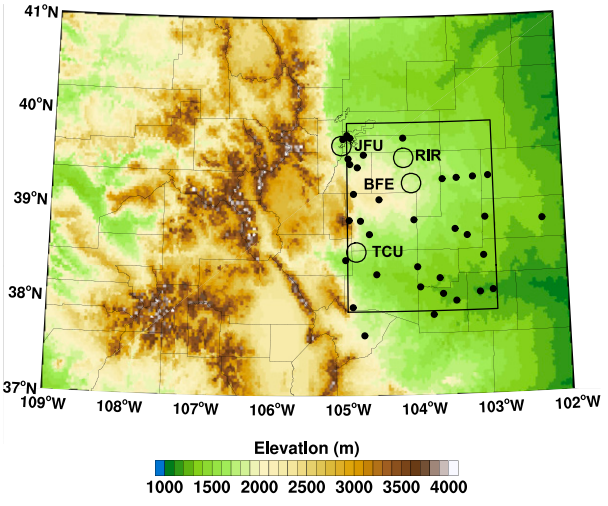


FIG. 2. This map locates the ponderosa pine stands used to develop the adjusted latewood width chronologies (open circles labeled BFE, JFU, RIR, TCU and defined in text). The black dots are the locations of the 40 instrumental precipitation stations. The box outlines the study area where the 72 grid points were used to compute the regional average daily precipitation totals for eastern Colorado (37.75°–39.75°N, 105°–103°W).

daily precipitation totals. Daily atmospheric data derived from the NCEP–NCAR reanalysis project (Kalnay et al. 1996) were used to identify synoptic-scale circulation features associated with the largest reconstructed 1-day rainfall totals over eastern Colorado. Because many of the station records begin after 1940, we restrict our analyses of the individual station observations to the period 1940–2019. Anomalies in the reanalysis data were calculated relative to the 1981–2010 climatology.

### b. *Eastern Colorado study region and adjusted latewood chronology development*

The range of ponderosa pine extends sparsely eastward from the Rocky Mountain Front Range into the Black Forest region of eastern Colorado. Native stands with old trees can occasionally be found on fire-protected escarpments and on certain higher elevation microenvironments (Wells 1965). Several annual ring-width chronologies of ponderosa pine have been previously developed in the study region and used to reconstruct spring PDSI and streamflow (Woodhouse and Brown 2001; Woodhouse and Lukas 2006). The annual growth ring for many temperature North American tree species is made up of several earlywood (EW) and latewood (LW) xylem cells that can be separately identified and measured each year. We remeasured four of these tree-ring collections for EW, LW, and total ring width (RW), and then computed the adjusted latewood width (LWa) chronologies for Black Forest East (BFE), Jefferson County (JFU), Ridge Road (RIR), and Turkey Creek (TCU; open circles in Fig. 2). These four sites are all located east of the continental divide, and range in elevation from 1800 (BFE) to 1965 m (JFU).

The following steps were used to compute the regional adjusted latewood width chronology for the eastern Colorado study region:

1) The previously collected and dendrochronologically dated core samples from four sites in Colorado (approximately 150 individual core specimens) were remeasured for EW, LW, and RW with a stage micrometer to 0.001 mm precision using the protocols outlined by Stahle et al. (2009).
2) Tree-ring chronologies of EW, LW, and RW width were computed for each site using the signal free method of standardization (Melvin and Briffa 2008; Cook et al. 2014). Power transformed ring-width indices were calculated as residuals from the fitted growth curve, and then averaged into the mean index chronology using the biweight robust mean (Cook 1985; Hoaglin et al. 2000).
3) Because the correlation between the EW and LW chronologies from a given site can be quite high (Torbenson et al. 2016), it is necessary to remove the dependency of LW on EW growth in order to derive separate estimates of summer precipitation from LW not dominated by spring climate and tree growth (Meko and Baisan 2001). These so-called adjusted latewood width chronologies are calculated via regression techniques (Meko and Baisan 2001) and represent the latewood growth variability that is independent of the EW. Therefore, these chronologies most likely represent the final latewood xylem cells of the annual ring formed at the end of the growing season. Adjusted latewood width chronologies for eastern Colorado were calculated using the Kalman filter (Welch and Bishop 2006) to allow for potential time-dependent variations in the relationship between EW and LW. In the case of North American conifers, LWa chronologies tend to be correlated *only* with summer precipitation totals (Meko and Baisan 2001; Stahle et al. 2009; Griffin et al. 2011, 2013; Crawford et al. 2015; Dannenberg and Wise 2016; Howard et al. 2019). However, this research in semiarid eastern Colorado indicates that LWa chronologies of ponderosa pine may be dominated by rainfall variability considerably shorter than the full summer season, in this case even at the daily time scale.
4) The variance for the four LWa chronologies had to be stabilized (Meko 1981) to account for changes in tree vigor with age and the declining sample size of dated ring width series in the beginning years of each chronology. A smoothing spline with a 50% frequency response equal to 100 years (Cook and Peters 1981) was fit to the absolute values of the annual LWa indices, and the ratios of the fitted spline to the absolute values were computed. The sign was then restored, and the mean added back to each annual value to produce the variance-stabilized LWa chronologies (Meko 1981; Cook and Krusic 2005).
5) The annual values for all four LWa chronologies were squared to increase skewness and better represent the distribution of the daily precipitation data for eastern Colorado.
6) The four adjusted latewood chronologies were then averaged for each year in common from 1779 to 1997 to produce the regional chronology used for the reconstruction of daily rainfall extremes in during this peak 2-week period in late July.

### c. *Daily precipitation response of the regional adjusted latewood chronology*

The gridded daily precipitation data were used to identify the highest correlation between the adjusted

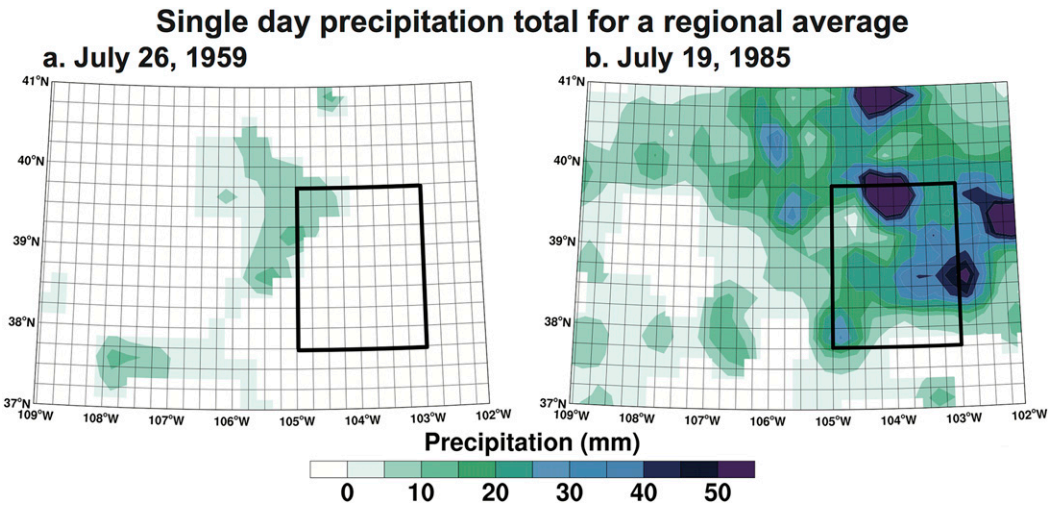


FIG. 3. These maps illustrate two different examples of the *wettest single-day precipitation total* during the 14-day interval from 19 Jul to 1 Aug for (a) 1959 and (b) 1985. The precipitation totals calculated from the 72 gridpoint regional average of the daily data were 1.35 and 25.67 mm for 26 Jul 1959 and 19 Jul 1985, respectively. These wettest days were identified each year to derive the annual time series of the single wettest day occurring in late July for eastern Colorado.

latewood width chronology and various daily to seasonal precipitation totals in eastern Colorado. The calculation of these daily to near-annual response profiles is summarized as follows:

1) The daily precipitation data were regionally averaged for the 72 grid points in eastern Colorado. The regional average daily data were then totaled for all possible intervals from 2 to 365 days ($n = 364$) throughout the year (e.g., the 2-day total for 1 January represents precipitation summed from 31 December to 1 January; 31 December is equal to the 2-day total for 30–31 December). This produces a total of 132 860 annual time series (364 possible intervals multiplied by 365 days).
2) The accumulated precipitation totals for all intervals from 2 to 365 days were correlated with the adjusted latewood chronology for every day of the year, and the correlation coefficients were calculated for all 365 Julian days.
3) All possible 1- to 31-day intervals during the year were used to identify the wettest single day in the given interval, producing a total of 11 315 annual time series (31 intervals multiplied by 365 days). Using the 14-day interval in late July as an example (i.e., 19 July to 1 August), the largest single-day total in 1959 for this interval occurred on 26 July (Fig. 3a). The value of 1.35 mm represents the regional averaged value and the wettest 24-h total for the 14-day period from 19 July to 1 August 1959. For the year 1985, the highest 24-h rainfall total in late July was 25.67 mm and occurred on 19 July (Fig. 3b). Note that for correlation with the tree-ring data, the optimal period for the wettest single day in all possible intervals turned out to be only 14-days long in midsummer (Fig. 4a).
4) The wettest single day in every possible 14-day interval during the year was correlated with the regional LWa chronology, and the correlation coefficients were plotted by Julian day (red line in Fig. 4a). For all possible 365 Julian days, the wettest day could be the same day for overlapping 14-day intervals. But for any given 2-week interval there was just 1 wettest day in that 14-day period.
5) The regional LWa correlation with regionally averaged precipitation totals *accumulated* for 7, 14, 21, 28, 35, 42, 49, and 56 days was also plotted by Julian day to compare with the correlations with the wettest single-day totals (gray lines in Fig. 4a)
6) The various 2- to 365-day accumulated precipitation totals were also correlated with the regional EW, LW, and RW chronologies to compare their seasonal response with the adjusted latewood chronology (Fig. 5).

### *d. Tree-ring reconstruction of 1-day precipitation extremes in midsummer*

Because the regional LWa chronology was best correlated with the wettest single day in the last two weeks of July (19 July–1 August), it was calibrated with a time series based on the wettest 24-h period from 19 July to 1 August for the common interval 1948–97. A secondary

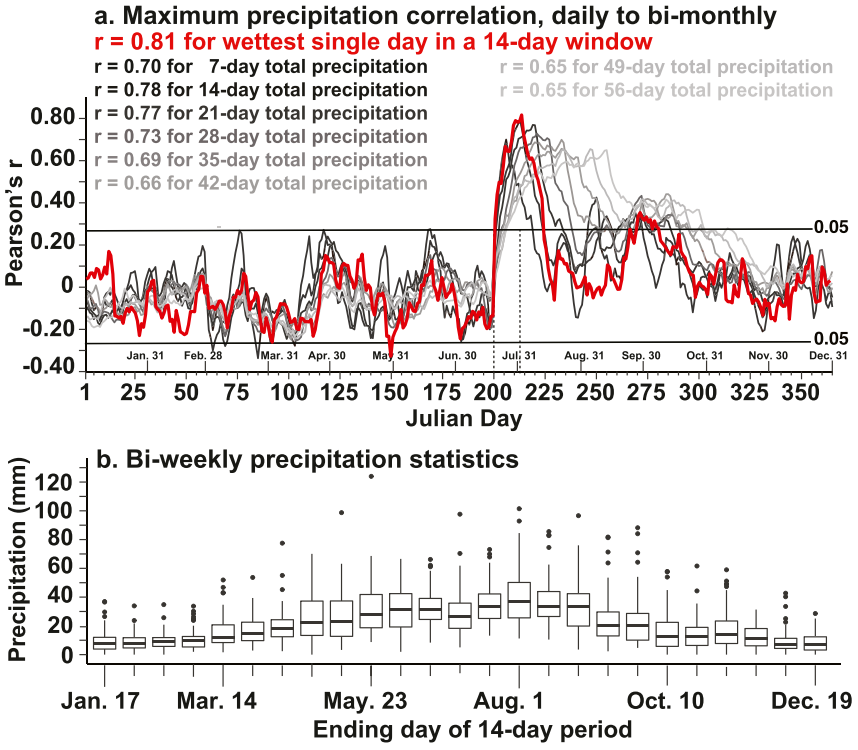


FIG. 4. (a) The correlations between the regional LWa chronology and the *wettest single-day precipitation total* over the eastern Colorado study area during overlapping 14-day intervals (i.e., each period overlaps the previous by 13 days) from 1948 to 1997 are plotted by Julian date of the year (red line). The $p < 0.05$ significant thresholds are noted (horizontal black lines). The correlations computed are for 50 years of data (1948–97) and correlation values above 0.273 and below −0.273 are considered significant at the $p < 0.05$ level. The highest correlation was computed for the wettest daily total during the 14-day interval extending from Julian day 200 to 213 (19 Jul to 1 Aug; $r = 0.81$). The vertical dashed lines denote this best 14-day interval (correlations are plotted at the end date of each 14-day interval). The correlation between the regional LWa chronology and precipitation *totals* accumulated for all possible 7 to 56 day periods during the year are also plotted (grayscale). The highest LWa correlation with 14-day *total* rainfall is also from Julian day 200 to 213 ($r = 0.78$), but is still below the correlation with the single wettest day during this interval ($r = 0.81$). (b) Box and whisker plots of the nonoverlapping biweekly precipitation climatology for the study area. The mean, upper, and lower quartiles are plotted in each box, along with the highest extreme values (dots; 1948–2019). Note that the highest 2-week mean precipitation also corresponds with the 2-week interval in (a) when the regional LWa chronology is most highly correlated with daily precipitation (i.e., late July).

instrumental time series of the wettest single day in late July was also extracted for eastern Colorado based on the grid point that contained the largest precipitation value each year from 19 July to 1 August. The regionally averaged time series was rescaled to this secondary series using simple linear regression, and the fitted values represent 24 h precipitation totals similar to the mean and magnitude of extreme rains that occur at localized scales over eastern Colorado. Rescaling the time series in this manner also prevented negative values from being estimated in the tree-ring reconstruction.

Since the tree-ring data end in 1997, the reconstruction was calibrated on the 50-yr period from 1948 to 1997. Separate calibration and validation experiments were performed for two subperiods during 1948–72 and 1973–97. The regional latewood chronology was first calibrated with the instrumental series using regression from 1973 to 1997, and the instrumental data from 1948 to 1972 were withheld for independent validation of the reconstruction. The regional LWa chronology was also calibrated on the earlier period, and the estimates were then independently validated on the later period. Because the coefficients of these two regression-based calibration models are similar, the final reconstruction was based on the full time period in common to the instrumental rainfall and adjusted latewood width data,

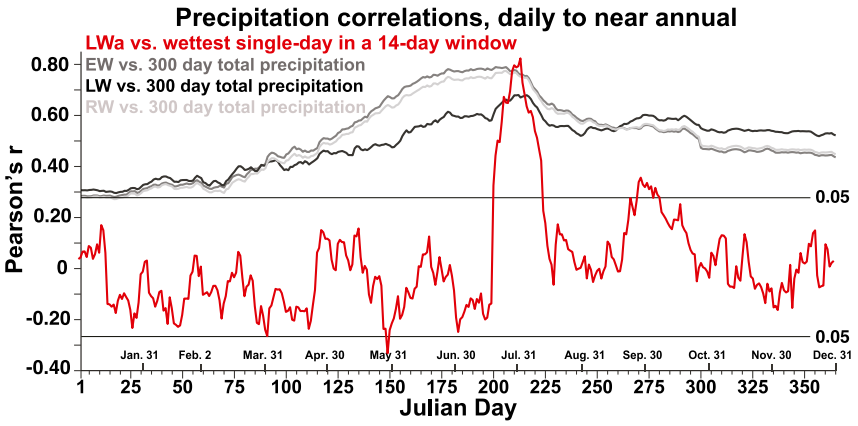


FIG. 5. The correlation of the regional LWa chronology with the wettest single day in all possible overlapping 14-day intervals from 1948 to 1997 peaks in late July (red line; from Fig. 4a) and is compared with the correlations between the regional chronologies of EW, LW, and RW for eastern Colorado for all possible continuous 300-day precipitation totals throughout the year (grayscale lines). The gridded daily precipitation data were totaled for all 300-day intervals beginning in the previous year and ending on the Julian date noted on the *x* axis during the current year for 1948–97 (1 Jan = previous Julian day 66 to current day 1). Note the strong near-annual precipitation signals integrated in the EW, LW, and RW chronologies, all of which include significant correlations during winter, spring, and summer. However, the LWa chronology is strongly correlated with single-day precipitation totals only in late July.

1948–97. The variance lost in the regression was restored to the reconstructions from 1779 to 1997 and the instrumental values were then appended to the estimates to complete the full reconstructed and instrumental time series from 1779 to 2019.

## 3. Results

The regional adjusted latewood chronology is significantly correlated with July precipitation totals for eastern Colorado ($r = 0.68$, $p < 0.0001$), but the correlation with the time series of the highest 1-day rainfall amount during the last two weeks of July is actually much stronger ($r = 0.81$, $p < 0.0001$; Fig. 4a). The correlation coefficients computed between the regional LWa chronology and the single highest daily precipitation total for all possible 14-day intervals during the year are plotted in Fig. 4a (the correlation for Julian day 1 is with the highest daily total between 19 December and 1 January). These correlations peak on Julian day 213 when the Pearson correlation with the wettest day in the 2-week interval reaches $r = 0.81$ (Spearman correlation is $r = 0.73$; not shown). Note the sharp increase in correlations at Julian day 200, indicating that this regional LWa chronology begins to be significantly correlated with the heaviest 1-day rainfall totals in the second week of July, even though the peak response is during the interval from Julian day 200–213, or 19 July–1 August (Fig. 4a). When the same method is applied using the 40 individual weather stations (black dots in Fig. 2), the highest correlation is also with the wettest daily total identified from 19 July to 1 August each year ($r = 0.77$; not shown). The overall highest correlation is in fact with the single wettest day identified at an individual grid cell each year ($r = 0.83$; not shown) instead of a regional average. However, the regionally averaged precipitation time series was used in calibration with the tree-ring data because the regional average more likely captures precipitation that impacted at least one tree-ring sample site and one or more instrumental rainfall recording stations in eastern Colorado.

For comparison with the response to 1-day precipitation during the last 2 weeks of July, the LWa chronology was also correlated with 1- to 8-week precipitation *totals* during the year (i.e., 7- to 56-day total precipitation; Fig. 4a). The highest correlation was computed for 14-day total precipitation during the same interval from 19 July to 1 August ($r = 0.78$; Fig. 4a). The correlations with 3- to 8-week totals then decline with increasing duration, but they all exhibit a July–August peak. The shortest 1-week total is only correlated at $r = 0.70$ in late July, which may indicate that 7 days is not a long enough window to capture the most intense storms of midsummer that influence tree growth. Note also that a modest secondary peak in correlation is present in September for all averaging intervals (Fig. 4a), and if real might represent a response to intense rain from upslope flow very late in warm season.

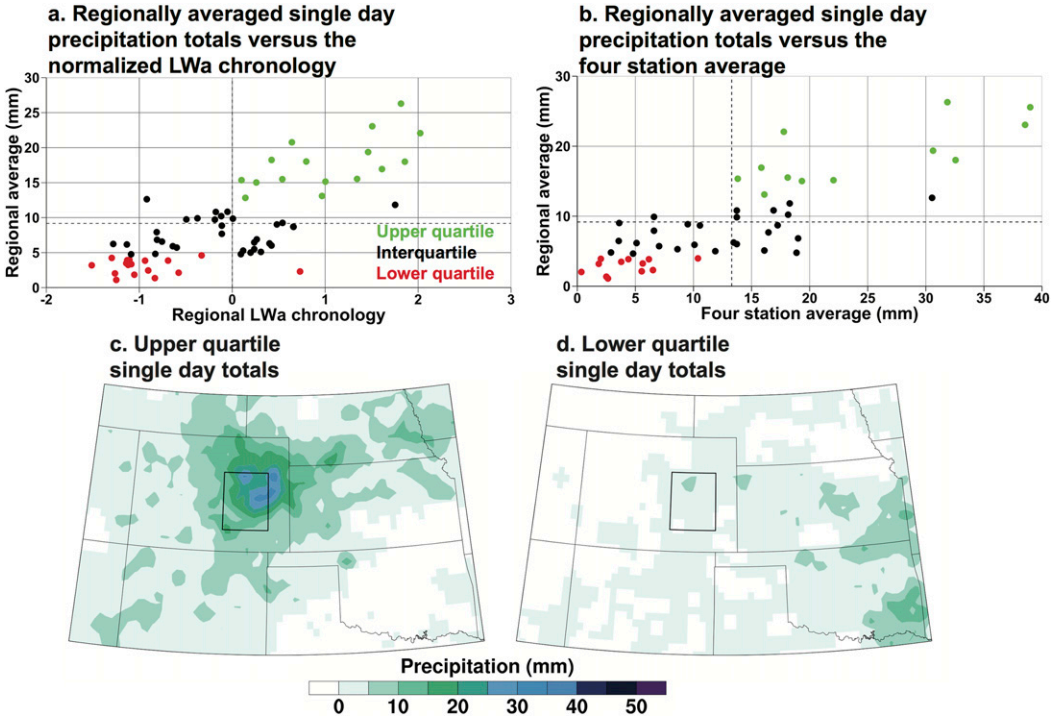


FIG. 6. (a) This scatterplot between instrumental single-day precipitation totals and the normalized LWa chronology for eastern Colorado illustrates the importance of rainfall extremes in the upper and lower quartiles [upper quartile (green), interquartile (black), and the lower quartile (red)]. (b) As in (a), but using the wettest day identified in the instrumental four-station average of daily precipitation totals as the dependent variable. The instrumental precipitation totals are averaged for (c) the upper ($n = 13$) and (d) the lower quartile events ($n = 12$) for late July from 1948 to 1997.

The high correlation with the single-day rainfall totals in late July coincides with the annual 2-week precipitation maximum over eastern Colorado (Fig. 4b). The average 2-week precipitation total from 19 July to 1 August is higher than every other possible 2-week period during the year (e.g., Fig. 4b). On average, nearly 70% of the total precipitation recorded in late July is contributed by the heaviest single rainfall day in this area (i.e., 68.25%). In fact, when analyzed at the grid point level for eastern Colorado, *all* of the 14-day total can be attributed to a single rain event during some years. The wettest 24 h period in a given year can occur outside the 19 July to 1 August period, of course, but it is within this 2-week period in late July when single-day precipitation totals tend to be heaviest (Fig. 1) and have the highest correlation with the regional LWa chronology.

The precipitation response of EW, LW, and RW is strikingly different than LWa in eastern Colorado (Fig. 5). The EW, LW, and RW chronologies have an integrated, nearly annual moisture signal and are most highly correlated with precipitation accumulated over several months prior to and during the growing season. These highest correlations with precipitation for all possible continuous intervals are accumulated over 305, 292, and 308 days during and preceding the growing season for the regional EW, LW, and RW regional chronologies. Using the precipitation response profile for 300-day total precipitation as an example, the highest correlation with both EW and RW is with precipitation totaled from the previous mid-September to current mid-July (22 September to 20 July, or Julian day 266 of the prior year to day 201 of the current year). The highest 300-day moisture signal for unadjusted LW is only slightly later (i.e., 2 October to 31 July).

The strong relationship between the 1-day rainfall totals during the 2-week precipitation peak in late July and the regional LWa chronology is present despite the low correlations among the four LWa chronologies. The average correlation among these four chronologies is only $r = 0.34$ during the calibration period (1947–97) and $r = 0.28$ for the full common interval (1779–1997). However, the individual LWa chronologies are more highly correlated with the average gridded time series of the wettest

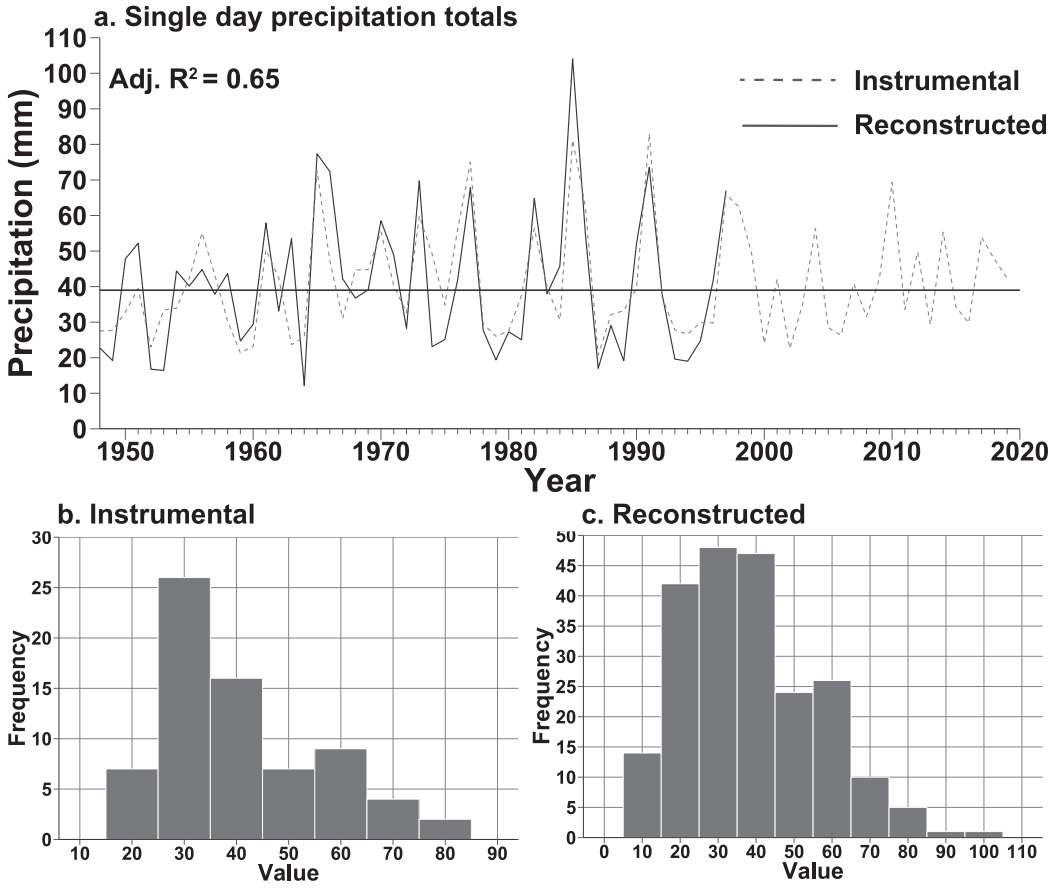


FIG. 7. (a) The instrumental and reconstructed highest single-day precipitation totals in midsummer are plotted from 1948 to 1997 (1998–2019 is instrumental data only for the 72-gridpoint regional average; instrumental mean also plotted). The reconstructed series are estimates after the variance lost in the regression has been restored. The frequency distributions of the (b) instrumental and (c) reconstructed highest single-day totals in late July are also illustrated, based on the periods 1948–2019 and 1779–1997, respectively.

single day during the last two weeks of July (range of $r = 0.44$ to 0.60 for the four chronologies). When these four LWa chronologies are averaged the correlation with the wettest single-day time series for eastern Colorado is $r = 0.81$.

The wettest single day in midsummer also tends to be rather weakly correlated among the instrumental rainfall stations [e.g., the four stations closest to the four tree-ring sites and with continuous daily precipitation daily (Denver, Byers, Limon, and Pueblo) are correlated on average at only $r = 0.25$ for the wettest day at each location from 19 July to 1 August, 1948–97, ranging from $r = 0.07$ to 0.65]. However, each of these four time series is positively correlated with the wettest single-day time series derived from the gridded data (range of $r = 0.54$ to 0.68 for the four stations). When the daily data are averaged among the four instrumental stations, and the wettest day is identified from this regional average (similar to what presumably happens at the four tree-ring collection sites), the correlation with the wettest single-day series based on the gridded data for eastern Colorado improves to $r = 0.84$. The regional LWa chronology is also highly correlated with the wettest day identified from a regional average of the four stations ($r = 0.70$).

These comparisons reflect the spatially discontinuous nature of summer precipitation events over eastern Colorado, but the common signal between the gridded data (or the weather stations) and the regional LWa chronology can be greatly enhanced with regional averaging. This strong relationship with single-day totals appears to be driven by the extreme years with the highest and lowest single-day totals. This is illustrated with a scatterplot between instrumental single-day precipitation totals and the normalized regional LWa chronology, highlighting the upper, inter, and lower quartiles from 1948 to 1997 (Fig. 6a). The correlation between the regional LWa chronology and just the

TABLE 1. (top) The calibration and validation statistics computed for the tree-ring reconstruction of 1-day precipitation totals in late July over eastern Colorado are listed. (bottom) The same statistics for an experimental reconstruction using an average of the largest 1-day rainfall totals among the four weather stations closest to the tree-ring collection sites are also listed (Byers, Denver, Limon, Pueblo; 19 Jul to 1 Aug). The statistics include the coefficient of determination, $R^2$, adjusted downward for loss of degrees of freedom (Draper and Smith 1981); the Pearson product moment correlation coefficient, $r$ (Draper and Smith 1981); reduction of error, RE (Fritts 2001); coefficient of efficiency, CE; and the root-mean-square error (RMSE; Cook and Kairiukstis 1990).

| Regional LWa chronology | | | | | | |
|---|---|---|---|---|---|---|
| Calibration period | Adjusted $R^2$ | Validation period | $r$ | RE | CE | RMSE |
| 1973–97 | 0.75 | 1948–72 | 0.75 | 0.51 | 0.49 | 11.00 |
| 1948–72 | 0.55 | 1973–97 | 0.87 | 0.71 | 0.70 | 11.28 |
| 1948–97 | 0.65 | — | — | — | — | 11.25 |

| Four station single-day precipitation totals in late July | | | | | |
|---|---|---|---|---|---|
| Calibration period | Adjusted $R^2$ | Validation period | $r$ | RE | CE |
| 1973–97 | 0.73 | 1948–72 | 0.78 | 0.66 | 0.59 |
| 1948–72 | 0.59 | 1973–97 | 0.86 | 0.74 | 0.72 |
| 1948–97 | 0.70 | — | — | — | — |

upper and lower quartiles of single-day precipitation is strong ($r = 0.88$; Fig. 6a), but the relationship with precipitation in the interquartile range is much weaker ($r = 0.38$; black circles in Fig. 6a). A similar relationship is found when comparing the gridded data and the wettest day based on a four station average of daily precipitation values (Fig. 6b). The correlation with the upper and lower quartiles ($r = 0.90$) is substantially higher compared to values closer to the mean ($r = 0.31$).

The notion that the extreme wet or dry midsummer conditions strongly influence the correlation with the regional LWa chronology is further supported by composites of the 24-h instrumental totals in the upper and lower quartiles from 1948 to 1997. The upper quartile composite corresponds with widespread precipitation over most of eastern Colorado and the central Great Plains, resembling frontally organized precipitation (Fig. 6c). This spatial pattern represents thunderstorm activity that might have impacted most if not all of the tree-ring sites used in calculation of the regional LWa chronology. The composite for the lower quartile events indicates that thunderstorm activity in late July was much less intense across eastern Colorado during these years and late season tree growth would likely have been limited by the lack of precipitation and soil moisture during this two week interval (Fig. 6d).

The reconstruction of midsummer 1-day rainfall extremes was developed using regression between the LWa chronology (predictor) and the single wettest day from 19 July–1 August for the eastern Colorado, using the 72-gridpoint regional average daily data (predictand). The instrumental and the reconstructed values are plotted in Fig. 7a. The reconstructed series explains 65% of the interannual variance in 1-day rainfall totals during the full 1948–97 calibration period (Fig. 7a). Split calibration and validation experiments on two 25-yr subperiods indicate the relationship between the two series is reasonably stable (Table 1, top). The instrumental and reconstructed rainfall distributions are positively skewed by the most extreme wet years (Figs. 7b,c).

For comparison with the tree-ring reconstruction, a wettest single-day time series computed for the peak 2-week period in late July from an average of the four closest rainfall stations was used to develop an alternative ''instrumental-only'' regression model. This four-station average of the wettest late July day was regressed with the 72-gridpoint regional average. The calibration and validation statistics calculated for this experimental instrument-only reconstruction are remarkably similar to the statistics based on the regional tree-ring data (Table 1, bottom), highlighting the fidelity of the tree-ring estimates.

The full 241-yr time series of reconstructed and instrumental data extends from 1779 to 2019 (instrumental data only from 1998 to 2019) and indicates interesting interannual to decadal variability of midsummer single-day rainfall extremes over eastern Colorado (Fig. 8). The frequency of the wettest >90th percentile events are estimated to have more than doubled from the nineteenth–twentieth centuries, while the driest <10th percentile events appear to have decreased since the late eighteenth century (Fig. 8). But in spite of the increase in wet extremes, stochastic volatility analysis (Kastner 2016) does not indicate a significant increase in the overall variance of the reconstructed or observed wettest 1-day totals (not shown).

The late twentieth century (1960–97) is estimated to have experienced a high frequency of 1-day rainfall extremes during in late July (Fig. 8). But there have been only two 90th percentile events since 1998 based on the

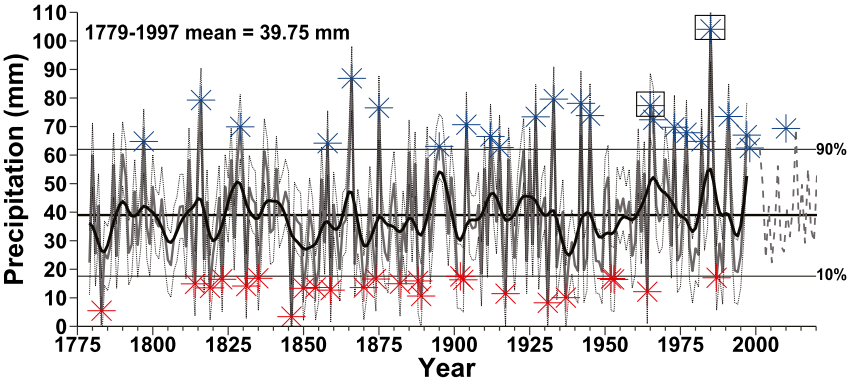


FIG. 8. The highest 1-day precipitation totals in late July were reconstructed from 1779 to 1997 (gray) and the instrumental data were appended from 1998 to 2019 (dashed). The full 1779–2019 time series is not a single homogeneous time series given the reconstruction contains uncertainty. Uncertainty is estimated based on the 80% confidence interval of the root-mean-square error (light gray lines; Table 1, top). A smoothed version of the reconstruction that highlights decadal variability is plotted in black from 1779 to 1997. The mean, 90th, and 10th percentile thresholds for 1779–2019 are plotted (horizontal lines) and extremes above or below these thresholds are noted (asterisks). Heavy precipitation days that were associated with significant flash flooding and severe weather in Colorado on 24 Jul 1965 and 19 Jul 1985 are also indicated (squares).

gridded instrumental data from 1998 to 2019 (1998 and 2010), and there have been no 10th percentile single-day totals over the same period. These changes are also evident in the daily precipitation data recorded at the 40 individual weather stations in eastern Colorado (Fig. 9). Many of the largest events identified in the instrumental data occur between the 1960s and 1990s, and there has been a noticeable decline in the heaviest midsummer precipitation days after 1999.

Major subdecadal to decadal periods of drought identified using instrumental and tree-ring reconstructed PDSI are also apparent in the 1-day late July rainfall totals [e.g., early twenty-first century, Seager (2007); 1930s Dust Bowl, Worster (1979); mid-nineteenth-century drought; Woodhouse et al. (2002); Herweijer et al. (2006); Cook et al. (2007); Fig. 8]. The Dust Bowl drought in particular had a negative impact on the highest rainfall totals during the 2-week precipitation maximum in late July over eastern Colorado. A total of 8 out of the 10 years from 1931 to 1940 are estimated to have been below average, and the only comparable period of sustained deficits in these single-day totals occurred during the 1840s and 1850s. The reconstruction of midsummer 1-day rainfall is not

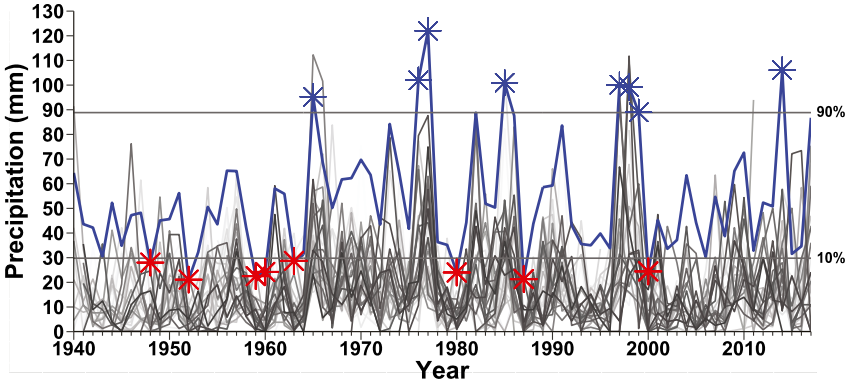


FIG. 9. The highest single-day precipitation totals identified at the 40 instrumental weather stations during late July are plotted individually from 1948 to 2019 (i.e., 19 Jul to 1 Aug; grayscale). A time series of the wettest day based on an average of the daily data for the 40 stations is also plotted (thick blue line) after being rescaled to the time series of the highest daily precipitation total identified from all 40 stations each year. Extremes above or below the 90th and 10th percentile thresholds are indicated for the regional average (asterisks).

correlated with a collocated regional average of reconstructed summer PDSI derived from the North American Drought Atlas (Cook et al. 2007) at interannual time scales ($r = 0.07$ from 1779 to 1997; not shown), but as these major PDSI droughts suggest, prolonged dryness appears to be associated with reduced daily rainfall extremes in late July. The decadal estimates of the wettest single-day time series is also not strongly correlated with decadal estimates of reconstructed PDSI ($r = 0.37$), but agreement among these smoothed time series is highest during the most severe and sustained droughts in the regional PDSI reconstructions.

The largest instrumental and reconstructed single-day extremes during the 1948–97 calibration period represent widespread precipitation events that impact much of eastern Colorado (Fig. 6c), and some of these events were connected with intense flash flooding and severe weather outbreaks. For example, the single-day total for 19 July 1985, is the largest estimated event since the late eighteenth century and is considered one of the wettest days in Colorado's history (Doesken and McKee 1986). Hourly rainfall rates recorded at many stations in eastern Colorado were greater than 25.4 mm on 19 July 1985, and widespread reports of flash flooding and other severe weather hazards including hail, damaging wind, and tornadoes are documented (Doesken and McKee 1986). The reconstructed heavy rainfall day for 24 July 1965, was part of a persistent pattern of widespread precipitation from 20 to 25 July, including heavy rains on 23–24 July that led to significant flash flooding of Tucker Gulch in Golden, Colorado. The 1976 Big Thompson Canyon flood and the 1997 Fort Collins event were not identified as extreme single-day events for eastern Colorado in either the instrumental or reconstructed data, but these storms and floods were located north of the study region. It is possible that the heavy 1-day rainfall events that led to the flash flooding of Big Thompson and Spring Creek near Fort Collins were recorded in adjusted latewood chronologies of ponderosa pine trees located within or near the vicinity of these drainage basins.

The synoptic meteorology of the five largest reconstructed single-day rainfall extremes is illustrated in Fig. 10. The most common synoptic pattern for these extreme events includes a surface high north of Colorado and a frontal boundary located over the central United States (Figs. 10a,c,e,g,i). Previous flash floods in eastern Colorado have been linked to strong frontal systems that move south of the region and create postfrontal easterly upslope flow behind the front (Petersen et al. 1999). Precipitable water value anomalies from the surface to 500 mb also indicate a deep layer of atmospheric moisture, which tends to increase the efficiency

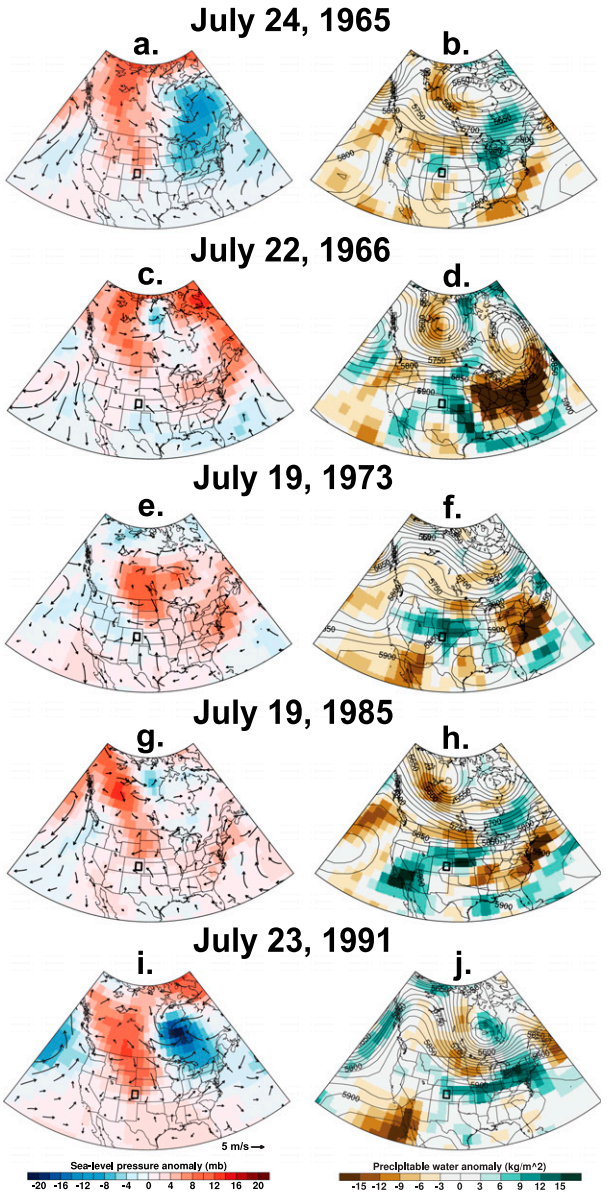


FIG. 10. The surface pressure anomaly (mb; shaded) and surface wind speed and direction (m s$^{-1}$; wind vectors) for the five highest reconstructed single-day precipitation totals in late July from 1948 to 1997 are shown for (a) 24 Jul 1965, (c) 22 Jul 1966, (e) 19 Jul 1973, (g) 19 Jul 1985, and (i) 23 Jul 1991. Note the large region of anomalous high pressure north of Colorado extending into Canada, and the area of low level wind convergence over the central United States for all events. (b),(d),(f),(h),(j) Mean 500 mb geopotential heights (contours) and the precipitable water value anomalies (kg m$^{-2}$) calculated from the surface to 500 mb are mapped for these five most extreme wet days of late July.

of precipitation (Figs. 10b,d,f,h,j). The 500 mb geopotential height patterns vary, but these large precipitation events are often associated with a moderate to strong upper-level ridge over Colorado (Figs. 10b,d,h), or a northwest-tilted ridge that extends from the Great

Plains to Pacific Northwest (Figs. 10f,j). The northwest tilted ridge axis (i.e., the bent-back ridge described by Maddox et al. 1978) has been previously identified as a key upper-level feature for previous flash flooding events in Colorado, including the 1976 Big Thompson Canyon flood and the 1997 flooding of Fort Collins (Maddox et al. 1978; Petersen et al. 1999; Cotton et al. 2003). The general synoptic meteorological features shown in Fig. 10, have been linked to widespread and extreme heavy rainfall over eastern Colorado during late July and early August (Doswell 1980; Maddox et al. 1980; Petersen et al. 1999; Cotton et al. 2003).

## 4. Discussion and conclusions

These results demonstrate that the precipitation response of ponderosa pine tree-ring chronologies can span a large range of time scales, from the annually integrated precipitation signal of total ring width to the daily precipitation extremes recorded by some adjusted latewood width chronologies. The seasonal to annual precipitation signal recorded by total ring-width chronologies has been widely applied, and this long-term integration of climate signal in ring-width data has been the ruling paradigm of dendroclimatology for 100 years (Douglass 1920). However, adjusted latewood width chronologies of ponderosa pine from eastern Colorado are highly correlated with precipitation at the daily time scale and demonstrate the feasibility for the tree-ring reconstruction of weather time-scale precipitation totals, or dendrometeorology.

The precipitation signals recorded by the last formed latewood cells in ponderosa pine, or other tree species in North America, have not been thoroughly explored. The few studies that have used adjusted latewood chronologies for moisture reconstruction have been calibrated with monthly or seasonal moisture data (e.g., Stahle et al. 2009, 2015; Griffin et al. 2013). Adjusted latewood chronologies also represent just one of several types of tree-ring data that partition the annual growth ring into subseasonal time scales. Subannual tree-ring data derived with X-ray densitometry (Schweingruber et al. 1978), blue-light intensity (Campbell et al. 2007), or stable isotopes (McCarroll and Loader 2004) might potentially record precipitation variability at the daily or weekly time scale, especially in semiarid regions where single events dominate the seasonal totals.

In an investigation of more than 300 heavy 1-day precipitation events for Colorado since the late nineteenth century, McKee and Doesken (1997) found that extreme rainfall can occur anywhere in Colorado typically from April through October, but there is a distinct peak of occurrence during the last week of July and first few days of August. The heaviest of these events most commonly occur in the foothills just east of the Rocky Mountains (McKee and Doesken 1997. Our results also indicate that the average two week precipitation total from 19 July to 1 August is highest compared to all possible two week intervals for the foothills and mainly the eastern High Plains of Colorado, and this precipitation maxima is largely the product of heavier single-day rainfall totals (Fig. 1). These single-day precipitation events, particularly the heaviest days when rainfall is widespread (Fig. 6c), may be the most important source of soil moisture recharge needed for late season tree growth of the ponderosa pine woodlands native to the Rocky Mountain Front Range and foothills of Colorado. Oxygen isotope measurements of the nearly full latewood from mature ponderosa pine in northern Arizona indicate a reliance on winter moisture (Kerhoulas et al. 2017), which is a similar finding to the results shown for the unadjusted latewood width data in Fig. 5. The response to single-day rainfall events during the wettest two week period of the year over eastern Colorado was only revealed after using the Kalman filter to isolate the last-formed xylem cells at the end of the growing season, which are represented by tree-ring chronologies of adjusted latewood width.

The reconstruction developed in this study does not estimate the largest single-day precipitation totals for the entire year, and in fact there have been a number of extreme precipitation events in Colorado that have led to significant flooding that cannot be captured by ponderosa pine adjusted latewood chronologies (e.g., the event in September 2013). However, the reconstruction does provide a valuable long-term perspective on heavy rains during a 2-week interval when extreme rains and severe weather occur with the highest probability (Weaver and Doesken 1990; McKee and Doesken 1997). The reconstruction estimates that heavy midsummer rainfall events increased from the late eighteenth century to the late twentieth century, with the period from 1960 to 1997 having the highest frequency of these extremes over the last 241 years. A time series of maximum 24 h precipitation totals for the entire year based on station observations for Denver also seems to indicate that the heaviest 24-h events for the entire year were on average larger in the mid- to late twentieth century compared to previous periods (McKee and Doesken 1997). Coupled with rapid urban development along the Front Range, some of the heavy rainfall extremes that occurred in summer led to costly flash flooding during the late twentieth century. Providing a long-term context for the frequency and magnitude of these extreme midsummer precipitation events across

many of the vulnerable Front Range drainage basins may now be possible based on the findings of this study. Ponderosa pine and other semiarid conifer species are native to many of the eastern Rocky Mountain and Front Range drainage basins that have been impacted by severe summer flash flooding, including the Big Thompson Canyon and Spring Creek near Fort Collins. Development of adjusted latewood width chronologies in these vulnerable basins could help investigate changes in the frequency of precipitation extremes in July and August over the last several hundred years.

*Acknowledgments.* The National Science Foundation funded this study (Grants AGS-1266014 and AGS-1702894). We thank Connie Woodhouse and Peter Brown for access to their collections, as well as Ed Cook, Dan Griffin, Dorian Burnette, Song Feng, John Tipton, and Max Torbenson for advice and assistance. We also would like to thank the Mandala Center in Des Moines, New Mexico, for permission to conduct fieldwork.

## REFERENCES

Alexander, M. A., J. D. Scott, K. Mahoney, and J. Barsugli, 2013: Greenhouse gas–induced changes in summer precipitation over Colorado in NARCCAP regional climate models. *J. Climate*, **26**, 8690–8697, https://doi.org/10.1175/JCLI-D-13-00088.1.

Barbosa, A. C. M. C., D. W. Stahle, D. J. Burnette, M. C. A. Torbenson, E. R. Cook, M. J. Bunkers, G. Garfin, and R. Villalba, 2019: Meteorological factors associated with frost rings in Rocky Mountain Bristlecone Pine at Mt. Goliath, Colorado. *Tree-Ring Res.*, **75**, 101, https://doi.org/10.3959/1536-1098-75.2.101.

Blasing, T. J., and H. C. Fritts, 1976: Reconstructing past climatic anomalies in the North Pacific and western North America from tree-ring data. *Quat. Res.,* **6**, 563–579, https://doi.org/10.1016/0033-5894(76)90027-2.

Bräuning, A., M. De Ridder, N. Zafirov, I. García-González, D. P. Dimitrov, and H. Gärtner, 2016: Tree-ring features: Indicators of extreme event impacts. *IAWA J.*, **37**, 206–231, https://doi.org/10.1163/22941932-20160131.

Campbell, R., D. McCarroll, N. J. Loader, H. Grudd, I. Robertson, and R. Jalkanen, 2007: Blue intensity in *Pinus sylvestris* tree-rings: Developing a new palaeoclimate proxy. *Holocene*, **17**, 821–828, https://doi.org/10.1177/0959683607080523.

Chen, M., W. Shi, P. Xie, V. B. S. Silva, V. E. Kousky, R. W. Higgins, and J. E. Janowiak, 2008: Assessing objective techniques for gauge-based analyses of global daily precipitation. *J. Geophys. Res.*, **113**, D04110, https://doi.org/10.1029/2007JD009132.

Cook, E. R., 1985: A time series analysis approach to tree-ring standardization. Ph.D. dissertation, University of Arizona, 171 pp.

——, and K. Peters, 1981: The smoothing spline: A new approach to standardizing forest interior tree-ring width series for dendroclimatic studies. *Tree-Ring Bull.*, **41**, 45–53.

——, and L. A. Kairiukstis, 1990: *Methods of Dendrochronology*. Kluwer Academic Publishers, 394 pp.

——, and J. P. Krusic, 2005: Program ARSTAN: A tree-ring standardization program based on detrending and autoregressive time series modeling with interactive graphics. Lamont-Doherty Earth Observatory, Columbia University, Palisades, NY.

——, R. Seager, M. A. Cane, and D. W. Stahle, 2007: North American drought: Reconstructions, causes, and consequences. *Earth-Sci. Rev.*, **81**, 93–134, https://doi.org/10.1016/j.earscirev.2006.12.002.

——, P. J. Krusic, and T. M. Melvin, 2014: Program RCSigFree. Tree-Ring Lab, Lamont Doherty Earth Observatory of Columbia University, Palisades, NY.

Cotton, W. R., R. L. McAnelly, and T. Ashby, 2003: Development of new methodologies for determining extreme rainfall: Final report for contract ENC C154213. Dept. of Natural Resources, State of Colorado, 140 pp., https://rams.atmos.colostate.edu/precip-proj/reports/112001/Cottonrpt1101.htm.

Crawford, C. J., D. Griffin, and K. F. Kipfmueller, 2015: Capturing season-specific precipitation signals in the northern Rocky Mountains, USA, using earlywood and latewood tree rings. *J. Geophys. Res. Biogeosci.*, **120**, 428–440, https://doi.org/10.1002/2014JG002740.

Dannenberg, M. P., and E. K. Wise, 2016: Seasonal climate signals from multiple tree ring metrics: A case study of *Pinus ponderosa* in the upper Columbia River Basin. *J. Geophys. Res. Biogeosci.*, **121**, 1178–1189, https://doi.org/10.1002/2015JG003155.

Doesken, N. J., and T. B. McKee, 1986: Colorado climate water-year series (October 1984–September 1985). Climatology Rep. 86-1, Department of Atmospheric Science, CSU, Fort Collins, CO, June, 115 pp.

——, and ——, 1998: An analysis of rainfall for the July 28, 1997 flood in Fort Collins, Colorado. Climatology Rep. 98-1, Department of Atmospheric Science, CSU, Fort Collins, CO, February, 55 pp.

Doswell, C. A., 1980: Synoptic-scale environments associated with High Plains severe thunderstorms. *Bull. Amer. Meteor. Soc.*, **61**, 1388–1400, https://doi.org/10.1175/1520-0477(1980)061<1388:SSEAWH>2.0.CO;2.

Douglass, A. E., 1920: Evidence of climatic effects in the annual rings of trees. *Ecology*, **1**, 24–32, https://doi.org/10.2307/1929253.

Draper, N., and H. Smith, 1981: *Applied Regression Analysis*. 2nd ed. John Wiley, 736 pp.

Edmondson, J. R., 2010: The meteorological significance of false rings in Eastern Redcedar (*Juniperus virginiana L.*) from the Southern Great Plains, U.S.A. *Tree-Ring Res.*, **66**, 19–33, https://doi.org/10.3959/2008-13.1.

Fritts, H. C., 2001: *Tree Rings and Climate*. Blackburn Press, 567 pp.

Gochis, D., and Coauthors, 2015: The great Colorado flood of September 2013. *Bull. Amer. Meteor. Soc.*, **96**, 1461–1487, https://doi.org/10.1175/BAMS-D-13-00241.1.

Griffin, D., and Coauthors, 2013: North American monsoon precipitation reconstructed from tree-ring latewood. *Geophys. Res. Lett.*, **40**, 954–958, https://doi.org/10.1002/grl.50184.

——, D. M. Meko, R. Touchan, S. W. Leavitt, and C. A. Woodhouse, 2011: Latewood chronology development for summer-moisture reconstruction in the US Southwest. *Tree-Ring Res.*, **67**, 87–101, https://doi.org/10.3959/2011-4.1.

Hales, J. E., 1974: Southwestern United States summer monsoon source—Gulf of Mexico or Pacific Ocean? *J. Appl. Meteor.*, **13**, 331–342, https://doi.org/10.1175/1520-0450(1974)013<0331:SUSSMS>2.0.CO;2.

Herweijer, C., R. Seager, and E. R. Cook, 2006: North American droughts of the mid to late nineteenth century: A history,

simulation and implication for Mediaeval drought. *Holocene*, **16**, 159–171, https://doi.org/10.1191/0959683606hl917rp.

Hoaglin, D. C., F. Mosteller, and J. W. Tukey, 2000: *Understanding Robust and Exploratory Data Analysis*. Wiley, 447 pp.

Hoerling, M. P., M. Dettinger, K. Wolter, J. Lukas, J. Eischeid, R. Nemani, B. Liebmann, and K. E. Kunkel, 2013: Present weather and climate: Evolving conditions. *Assessment of Climate Change in the Southwest United States: A Report Prepared for the National Climate Assessment*, G. Garfin et al., Eds., Island Press, 74–100.

Howard, I. M., D. W. Stahle, and S. Feng, 2019: Separate tree-ring reconstructions of spring and summer moisture in the northern and southern Great Plains. *Climate Dyn.,* **52**, 5877–5897, https://doi.org/10.1007/s00382-018-4485-8.

Kalnay, E., and Coauthors, 1996: The NCEP/NCAR 40-Year Reanalysis Project. *Bull. Amer. Meteor. Soc.*, **77**, 437–471, https://doi.org/10.1175/1520-0477(1996)077<0437:TNYRP>2.0.CO;2.

Karl, T. R., and R. W. Knight, 1998: Secular trends of precipitation amount, frequency, and intensity in the United States. *Bull. Amer. Meteor. Soc.*, **79**, 231–241, https://doi.org/10.1175/1520-0477(1998)079<0231:STOPAF>2.0.CO;2.

Kastner, G., 2016: Dealing with stochastic volatility in time series using the R Package stochvol. *J. Stat. Software*, **69** (5), https://doi.org/10.18637/jss.v069.i05.

Kerhoulas, L. P., T. E. Kolb, and G. W. Koch, 2017: The influence of monsoon climate on latewood growth of southwestern ponderosa pine. *Forests*, **8**, 140, https://doi.org/10.3390/f8050140.

Kunkel, K. E., L. E. Stevens, S. E. Stevens, L. Sun, E. Anssen, D. Wuebbles, K. T. Redmond, and J. G. Dobson, 2013: Regional climate trends and scenarios for the U.S. National Climate Assessment. NOAA Tech. Rep. NESDIS, 77 pp.

LaMarche, V. C., and K. K. Hirschboeck, 1984: Frost rings in trees as records of major volcanic eruptions. *Nature*, **307**, 121–126, https://doi.org/10.1038/307121a0.

Lukas, J., J. Barsugli, N. Doesken, I. Rangwala, and K. Wolter, 2014: Climate change in Colorado: A synthesis to support water resources management and adaptation. *A Report for the Colorado Water Conservation Board*, Western Water Assessment, 114 pp.

Maddox, R. A., L. R. Hoxit, C. F. Chappell, and F. Caracena, 1978: Comparison of meteorological aspects of the Big Thompson and Rapid City flash floods. *Mon. Wea. Rev.*, **106**, 375–389, https://doi.org/10.1175/1520-0493(1978)106<0375:COMAOT>2.0.CO;2.

——, F. Canova, and L. R. Hoxit, 1980: Meteorological characteristics of flash flood events over the western United States. *Mon. Wea. Rev.*, **108**, 1866–1877, https://doi.org/10.1175/1520-0493(1980)108<1866:MCOFFE>2.0.CO;2.

Mahoney, K. M., F. M. Ralph, K. Wolter, N. Doesken, M. Dettinger, D. Gottas, T. Coleman, and A. White, 2015: Climatology of extreme daily precipitation in Colorado and its diverse spatial and seasonal variability. *J. Hydrometeor.*, **16**, 781–792, https://doi.org/10.1175/JHM-D-14-0112.1.

——, J. J. Lukas, and M. Mueller, 2018: Colorado–New Mexico Regional Extreme Precipitation Study. Summary Report, Volume VI: Considering Climate Change in the Estimation of Extreme Precipitation for Dam Safety. Tech. Rep., Colorado Division of Water Resources and New Mexico Office of the State Engineer, 57 pp., https://wwa.colorado.edu/publications/reports/co-nm-reps_summary.pdf.

Matthai, H. F., 1969: Floods of June 1965 in South Platte River Basin Colorado. Water Supply Paper 1850— B, U.S. Geological Survey, Washington, DC, 64 pp.

McCarroll, D., and N. J. Loader, 2004: Stable isotopes in tree rings. *Quat. Sci. Rev.*, **23**, 771–801, https://doi.org/10.1016/j.quascirev.2003.06.017.

McKee, T. B., and N. J. Doesken, 1997: Colorado extreme storm precipitation data study: Final report. Climatology Rep. 97-1, Dept. of Atmospheric Science, Colorado State University, Fort Collins, CO, 109 pp., http://ccc.atmos.colostate.edu/pdfs/Climo_97-1_Extreme_ppt.pdf.

Meko, D. M., 1981: Applications of Box–Jenkins methods of time series analysis to the n reconstruction of drought from tree rings. Ph.D. dissertation, The University of Arizona, 149 pp.

——, and C. H. Baisan, 2001: Pilot study of latewood-width of conifers as an indicator of variability of summer rainfall in the North American monsoon region. *Int. J. Climatol.*, **21**, 697–708, https://doi.org/10.1002/joc.646.

Melvin, T. M., and K. R. Briffa, 2008: A ''signal-free'' approach to dendroclimatic standardisation. *Dendrochronologia*, **26**, 71–86, https://doi.org/10.1016/j.dendro.2007.12.001.

Palmer, W. C., 1965: Meteorological drought. U.S. Weather Bureau Research Paper 45, 58 pp.

Petersen, W. A., and Coauthors, 1999: Mesoscale and radar observations of the Fort Collins flash flood of 28 July 1997. *Bull. Amer. Meteor. Soc.*, **80**, 191–216, https://doi.org/10.1175/1520-0477(1999)080<0191:MAROOT>2.0.CO;2.

Schweingruber, F., H. Fritts, O. Braker, L. Drew, and E. Schar, 1978: The X-ray technique as applied to dendroclimatology. *Tree-Ring Bull.*, **38**, 61–91.

Seager, R., 2007: The turn of the century North American drought: Global context, dynamics, and past analogs. *J. Climate*, **20**, 5527–5552, https://doi.org/10.1175/2007JCLI1529.1.

Stahle, D. W., 1990: The tree-ring record of false spring in the southcentral United States. Ph.D. dissertation, Arizona State University, 272 pp.

——, and M. K. Cleaveland, 1992: Reconstruction and analysis of spring rainfall over the southeastern U.S. for the past 1000 years. *Bull. Amer. Meteor. Soc.*, **73**, 1947–1961, https://doi.org/10.1175/1520-0477(1992)073<1947:RAAOSR>2.0.CO;2.

——, and Coauthors, 2009: Cool- and warm-season precipitation reconstructions over western New Mexico. *J. Climate*, **22**, 3729–3750, https://doi.org/10.1175/2008JCLI2752.1.

——, J. R. Edmondson, J. N. Burns, D. K. Stahle, D. J. Burnette, E. Kvamme, C. Lequesne, and M. D. Therrell, 2015: Bridging the gap with subfossil Douglas-fir at Mesa Verde, Colorado. *Tree-Ring Res.*, **71**, 53–66, https://doi.org/10.3959/1536-1098-71.2.53.

Tang, M., and E. R. Reiter, 1984: Plateau monsoons of the Northern Hemisphere: A comparison between North America and Tibet. *Mon. Wea. Rev.*, **112**, 617–637, https://doi.org/10.1175/1520-0493(1984)112<0617:PMOTNH>2.0.CO;2.

Torbenson, M. C. A., D. W. Stahle, J. Villanueva Díaz, E. R. Cook, and D. Griffin, 2016: The relationship between earlywood and latewood ring-growth across North America. *Tree-Ring Res.*, **72**, 53–66, https://doi.org/10.3959/1536-1098-72.02.53.

Villalba, R., and T. Veblen, 1996: A tree-ring record of dry spring–wet summer events in the forest-steppe ecotone, northern Patagonia, Argentina. *Tree Rings, Environment and Humanity*, J. S. Dean, D. M. Meko, and T. W. Swetnam, Eds., Radiocarbon, 107–116.

Weaver, J. F., and N. J. Doesken, 1990: Recurrence probability—A different approach. *Weather*, **45**, 333–339, https://doi.org/10.1002/j.1477-8696.1990.tb05659.x.

Welch, G., and G. Bishop, 2006: An introduction to the Kalman filter. Tech. Rep. TR 95-041, Department of Computer Science, University of North Carolina at Chapel Hill, 16 pp.

Wells, P. V., 1965: Scarp woodlands, transported grassland soils, and concept of grassland climate in the Great Plains region. *Science*, **148**, 246–249, https://doi.org/10.1126/science.148.3667.246.

Woodhouse, C. A., and P. M. Brown, 2001: Tree-ring evidence for Great Plains drought. *Tree-Ring Res.*, **57**, 89–103.

——, and J. J. Lukas, 2006: Drought, tree rings and water resource management in Colorado. *Can. Water Resour. J.*, **31**, 297–310, https://doi.org/10.4296/cwrj3104297.

——, ——, and P. M. Brown, 2002: Drought in the western Great Plains, 1845–56: Impacts and implications. *Bull. Amer. Meteor. Soc.*, **83**, 1485–1494, https://doi.org/10.1175/BAMS-83-10-1485.

Worster, D., 1979: *Dust Bowl: The Southern Plains in the 1930s*. Oxford University Press, 304 pp.

Wuebbles, D. J., and Coauthors, 2017: Executive summary. *Climate Science Special Report: Fourth National Climate Assessment*, Volume I, 36 pp.

Xie, P., M. Chen, S. Yang, A. Yatagai, T. Hayasaka, Y. Fukushima, and C. Liu, 2007: A gauge-based analysis of daily precipitation over East Asia. *J. Hydrometeor.*, **8**, 607–626, https://doi.org/10.1175/JHM583.1.